International Journal of Modelling and Simulation, Vol. 23, No. 4, 2003

ANALYTICAL MODELLING OF FIBRE NONLINEARITIES IN AMPLIFIED DISPERSION COMPENSATED WDM SYSTEMS

I.B. Djordjevic,* A. Stavdas,** C. Skoufis,** S. Sygletos,** and C. Matrakidis**

Abstract

An analytic approach to calculation of Q-factor degradation due to the fibre nonlinearities in a wavelength-division multiplexing system is presented, as well as their interplay with dispersion and ASE noise accumulation. The derived expressions are applicable to any channel and any fibre type. The derivation of analytic solutions facilitates in studying and understanding complex optical communication systems in a way that is not possible using numerical simulations. The results suggested that the optimum selection of the power per channel could strongly depend on several system parameters. The model we have developed can be used in designing advanced WDM systems with a large number of channels spanning many amplification bands.

Key Words

Fibre Nonlinearities, Analytical modeling, WDM, Four Wave mixing (FWM), Cross Phase Modulation (XPM), Stimulated Raman Scattering (SRS), EDFA modeling, Q Factor

1. Introduction

The optical communication revolution based on Wavelength Division Multiplexing (WDM) is progressing at an astonishing rate. Transmission capacity throughput of 10 Tb/s has been reported [1], suggesting that the initial assumption of an unlimited capacity optical fibre is now questionable. Concurrently, the exploitation of optical amplification beyond the Erbium-Doped Fibre Amplifier (EDFA) in the C-band, through the proliferation of Raman amplifiers and agile optical multiplexing [2], marks the dawn of optical networking within the entire third-low-attenuation window of standard fibre [3]. The transmission engineering of such wavelength-rich networks requires in-depth understanding of the combined effect of fibre nonlinearities as well as their interplay with dispersion and the amplified spontaneous emission (ASE) noise accumulated due to the use of optical amplifiers.

The influence of nonlinearities on signal quality has been extensively studied during the last two decades [e.g., 4–16]. To date, fibre nonlinearities like Stimulated Raman Scattering (SRS), Cross Phase Modulation (XPM), and Four Wave Mixing (FWM) are primarily investigated independently of each other. Further, it is known that dispersion compensation has a different effect on the strength of each separate nonlinearity. In system studies, the optimum trade-off between dispersion penalty and nonlinearity penalty is sought, but a reliable conclusion cannot be drawn unless all nonlinearities are studied collectively. This is because it is possible that the parameter optimization adopted considering a single nonlinearity may degrade, instead of improving, the overall system performance. Current system studies that examine the overall outcome of all the aforementioned adverse effects are based on solving of the nonlinear Schrodinger equation numerically.

However, the role of analytical solutions is of primary importance for understanding the real behaviour of fibre nonlinearities, deriving system design guidelines as well as avoiding very cumbersome and time-consuming numerical simulations in multi-Tb/s applications. Here, the collective influence of SRS, FWM, and XPM on Q-factor degradation is studied for periodically amplified dispersion compensated links. The primary objective is to identify the conditions for which the overall effect of the nonlinearities is minimized. In the derivation, the following assumption has been made: the influence of one nonlinearity on the evolution of the others is very small and the beating of nonlinearities with ASE noise can be ignored, which was confirmed by experiments [20] to be valid in submarine systems, where the amplifier spacing is about 45 km and the average power per channel less than 0 dBm. We expect this approximation to be valid also in MAN and WAN applications. The assumption above will significantly sim-

* Department of Electrical & Electronic Engineering, Optical Communications Research Group, University of Bristol, Bristol, BS8 1TR UK; e-mail: icadj@yahoo.com or Ivan.Djordjevic@bristol.ac.uk

** Department of Electrical and Computer Engineering, National Technical University of Athens, Heroon Polytechniou 9, Zographou 15773, Athens, Greece; e-mail: astavdas@cc.ece.ntua.gr, harskouf@telecom.ece.ntua.gr, ssygl@cc.ece.ntua.gr, cmatraki@telecom.ece.ntua.gr

Recommended by Prof. M.Z. Atashbar
(paper no. 205-4016)

plify the complexity of the calculations. A schematic illustration of the point-to-point link is given in Fig. 1. A fibre link is comprised of a SMF segment of length L_1 followed by a DCF section of length L_2 and an optical amplifier that exactly compensates the fibre losses. A pre-emphasis filter that removes the deterministic part of SRS at the input of each optical amplifier (EDFA) is also assumed, implying that the input power per channel in all fibre links is the same. For studying fibre nonlinearities, one channel is considered to be the test channel and the rest interfering channels.

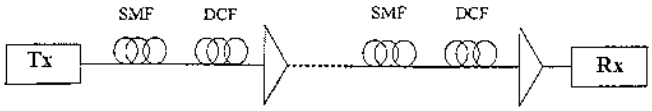

Figure 1. A distributed dispersion compensated WDM system.

In this work, the transmitter consists of a laser with an external modulator operating up to 10 Gb/s using Non-Return-to-Zero (NRZ) modulation format. Hence, if $P(i\omega)$ is the Fourier transform on an NRZ rectangular pulse of duration T, it is $P(i\omega) = P_0 T \frac{\sin(\omega T/2)}{\omega T/2} e^{-i\omega T/2}$ where P_o is the power of the pulse.

In Section 2 the modelling of SRS, FWM, and XPM is presented, and in Section 3 the assumptions used for calculating the Q-factor are presented, followed by the corresponding results.

2. Modelling of Fibre Nonlinearities

In subsequent sections the dispersion coefficient as a function of wavelength for the standard single-mode fibre (SMF) is given by:

$$D_{SMF}(\lambda) = \frac{S_0}{4}\lambda\left(1 - \frac{\lambda_0^4}{\lambda^4}\right) \tag{1}$$

with λ_0 and S_0 being the zero-dispersion wavelength and the dispersion slope at λ_0, respectively. The corresponding approximation for dispersion compensating fibre (DCF) is:

$$D_{DCF}(\lambda) = S_c(\lambda - \lambda_c) + D_c \tag{2}$$

with S_c and D_c being the dispersion slope and the dispersion at the wavelength $\lambda_c = 1550$ nm.

2.1 Modelling of SRS

SRS may limit the performance of a WDM system by depleting the lower wavelength channels [7–9]. In early SRS studies [e.g., 7] the worst-case scenario is assumed where all N channels are at the mark state simultaneously. This is very rarely true, and in any case the deterministic (mean value) part of the SRS degradation can be compensated, at least in principle, unlike the statistical crosstalk. Here both the mean value and the statistical variation are considered, but it is assumed that the former is compensated.

In [7] an exact analytical solution for SRS is given. However, the results hold only for the most affected channel, so the derived expressions are not directly applicable for an SMF/DCF link of two-fibre segments of lengths L_1 and L_2 with different effective cross-sectional areas (A_{e1}, A_{e2}), fibre attenuation coefficients (α_1, α_2), and Raman gain slopes (g_1', g_2'). Further, in [8] it is assumed that the dispersion compensated fibre (DCF) does not induce SRS. Here the derived expressions hold for any channel and the DCF contribution to SRS was also taken into account. However, the effect of pulse distortion, due to dispersion, on the SRS is ignored.

Assuming that the launched power is equal for all N channels, that is, $P_n(0) = P_0$ (n=1,2,...N), and if $g_1' = dg_1/df$ and $L_{e1} = (1 - e^{-a_1 L_1})/a_1$ are the Raman gain slope and the effective length of the SMF, then the power $P_n(L_1)$ of the n^{th} channel at the end of the SMF is given by [7]:

$$P_n(L_1) = NP_0 e^{-a_1 L_1} \frac{\exp\left[\frac{g_1' \Delta f N P_0 L_{e1}}{4A_{e1}}(2n - N - 1)\right] \sinh\left(\frac{g_1' \Delta f N P_0 L_{e1}}{4A_{e1}}\right)}{\sinh\left(\frac{g_1' \Delta f N^2 P_0 L_{e1}}{4A_{e1}}\right)} \tag{3}$$

However, the various channels at the input of DCF have different power levels. The expression for the power of the n^{th} channel at the end of DCF for nonequal channel launch powers, after [7], is:

$$P_n(L_1 + L_2) = \frac{P_n(L_1) J_0 e^{-\alpha_2 L_2} \exp\left[\frac{g_2' \Delta f J_0 (n-1) L_{e2}}{2A_{e2}}\right]}{\sum_{m=1}^{N} P_m(L_1) \exp\left[\frac{g_2' \Delta f J_0 (m-1) L_{e2}}{2A_{e2}}\right]} \tag{4}$$

where:

$$J_0 = \sum_{M-1}^{N} P_m(L_1)$$

The mean power depletion due to SRS, as measured on the n^{th} channel (the channel under test) at the end of a single link, is defined as:

$$\mu_D(n) = \frac{P_0 e^{-(a_1 L_1 + a_2 L_2)} - P_n(L_1 + L_2)}{P_0 e^{-(a_1 L_1 + a_2 L_2)}} \tag{5}$$

Equation (5), using (4), takes the form:

$$\mu_D(n) = \frac{1 - N \exp\left[-\frac{\Delta f N P_0}{2}\left(\frac{g'L}{2A}\right)_{eff}(N + 1 - 2n)\right] \sinh\left(\frac{\Delta f N P_0}{2}\left(\frac{g'L}{2A}\right)_{eff}\right)}{\sinh\left(\frac{\Delta f N^2 P_0}{2}\left(\frac{g'L}{2A}\right)_{eff}\right)} \tag{6}$$

where $\left(\frac{g'L}{2A}\right)_{eff} = \frac{g_1'}{2A_{e1}} \frac{1 - e^{-a_1 L_1}}{a_1} + e^{-a_1 L_1} \frac{g_2'}{2A_{e2}} \frac{1 - e^{-a_2 L_2}}{a_2}$,

Δf is the frequency channel spacing. To take into account the statistics of the transmitted symbols, the previous expression is multiplied with the probability of transmitting a bit on the mark-stage, which is taken as 0.5.

Using similar arguments with [8], the overall Raman crosstalk variance on the n^{th} channel at the end of the first SMF/DCF link is [9]:

$$\sigma_D^2(n) = \sum_{k=1, k\neq n}^{N} \sigma_k^2(n) \tag{7}$$

where $\sigma_k^2(n)$ is the SRS crosstalk variance of the n^{th} channel due to the interaction with the k^{th} channel. In turn, $\sigma_k^2(n)$ is:

$$\sigma_k^2(n) = \frac{1}{8\pi T} \int_{-\infty}^{\infty} \left| Q_k^{(n)}(\omega) \right|^2 d\omega \tag{8}$$

where $Q_k^{(n)}(\omega)$ essentially is the Fourier Transform of a pulse in the pulse train. It is:

$$\left|Q_k^{(n)}(\omega)\right|^2 = |P(i\omega)|^2 \left| \frac{K_1(n,k)\left(1-\exp\left[-\left(\alpha_1 - id_{k,n}^{(1)}\omega\right)L_1\right]\right)}{\alpha_1 - id_{k,n}^{(2)}\omega} + \right.$$

$$\left. \exp\left[-\left(\alpha_1 - id_{k,n}^{(1)}\omega\right)L_1\right] \frac{K_2(n,k)\left(1-\exp\left[-\left(\alpha_2 - id_{k,n}^{(2)}\omega\right)L_2\right]\right)}{\alpha_2 - id_{k,n}^{(2)}\omega} \right|^2$$

where $d_{12} \equiv (v_{g1})^{-1} - (v_{g2})^{-1} = \int_{\lambda_1}^{\lambda_2} D(\lambda)\, d\lambda$ is the walk-off parameter and $K_\rho(n,k) = g'_\rho(n-k)\,\Delta f/(2A_{e\rho})$, ($\rho$=1,2).

2.2 Modelling of Four-Wave-Mixing

Following the procedure described in [10, 11], the power of the new optical wave at frequency $f_{ijk} = f_i + f_j - f_k$ generated through the FWM nonlinear interaction of three channels with carrier frequencies f_i, f_j and f_k at the end of a single link is given by:

$$P_{ijk}(L_1 + L_2) =$$

$$\frac{1}{9} p_{ij} \gamma_1 \gamma_2 U_{ijk}^2 P_i(0) P_j(0) P_k(0) e^{-(a_1 L_1 + a_2 L_2)} \eta_{ijk} \tag{9}$$

where $P_i(0)$, $P_j(0)$, $P_k(0)$, are the input powers of the carriers with frequencies f_i, f_j, and f_k; $\gamma_\rho = 2\pi n^{(\rho)}/(\lambda A_e^{(\rho)})$ is the nonlinear coefficient of the corresponding fibre segment; $\rho = 1$ for SMF and $\rho = 2$ for DCF; n is the intensity-dependent refractive index; and U_{ijk} is the degeneracy factor that takes a value of 3 (for $i = j$) or 6 (for $i \neq j$). The factor p_{ij} comes from the fact that a new frequency is generated via FWM when two ($i = j$) or three channels ($i \neq j$) are simultaneously in the "mark" condition. The probability of this happening is taken as $(1/2)^2 = 1/4$ for $i = j$ and $(1/2)^3 = 1/8$ for $i \neq j$.

In (9) η_{ijk} is the FWM factor is given by:

$$\eta_{ijk} = \left| \frac{1 - e^{-(a_1 - i\Delta\beta_{ijk}^{(1)})L_1}}{a_1 - i\Delta\beta_{ijk}^{(1)}} \right.$$
$$\left. + e^{-(\alpha_1 - i\Delta\beta_{ijk}^{(1)})L_1} \frac{1 - e^{-(a_2 - i\Delta\beta_{ijk}^{(2)})L_2}}{a_2 - i\Delta\beta_{ijk}^{(2)}} \right|^2 \tag{10}$$

where $\Delta\beta_{ijk}^{(m)}$ represents the propagation constant difference (phase mismatch) $\Delta\beta_{ijk} = \beta_{ijk} + \beta_k - \beta_j - \beta_i$ between the carriers, and:

$$\Delta\beta_{ijk}^{(m)}(\lambda_n) = \frac{2\pi\lambda_n^2}{c}(f_i - f_k)(f_j - f_k)$$
$$\left\{ D^{(m)}(\lambda_n) + \frac{\lambda_n^2}{2c} \frac{dD^{(m)}(\lambda)}{d\lambda}\Big|_{\lambda=\lambda_n} [(f_i - f_n) + (f_j - f_n)] \right\},$$

where $D^{(m)}(\lambda_n)$ and $dD^{(m)}(\lambda)/d\lambda\big|_{\lambda=\lambda_n}$ are the dispersion and the dispersion slope of the m^{th} fibre segment for the n^{th} channel, respectively.

In a WDM system with N channels with equal channel spacing, the average FWM power generated at frequency f_n at the end of the M^{th} link, assuming that the input power per channel is constant ($P_l(0) = P_0, \quad l = 1, 2, \ldots, N$), can be written as follows [12]:

$$P_n = \frac{1}{9}\gamma_1\gamma_2 P_0^3 e^{-(a_1 L_1 + a_2 L_2)} \sum_{f_n = f_i + f_j - f_k}$$
$$p_{ij}\eta_{ijk}U_{ijk}^2 \frac{\sin^2\left[M\left(\Delta\beta_{ijk}^{(1)}(\lambda_n)L_1 + \Delta\beta_{ijk}^{(2)}(\lambda_n)L_2\right)/2\right]}{\sin^2\left[\left(\Delta\beta_{ijk}^{(1)}(\lambda_n)L_1 + \Delta\beta_{ijk}^{(2)}(\lambda_n)L_2\right)/2\right]}$$

$$(n, i, j, k = 1, 2, ..., N) \tag{11}$$

The summation in (11) is over all relevant combinations satisfying the relationship $f_n = f_i + f_j - f_k (k \neq i$ and $k \neq j)$. Obviously, (11) depends on the number of pulses in the "mark" position in a given time-slot, something that introduces a statistical approach.

2.3 Modelling of XPM

Cross-phase modulation (XPM) is an important source of performance degradation in multichannel WDM systems. This phenomenon arises from the dependence of the refractive index on the intensity of other optical waves via the Kerr effect. In the following the analysis presented in [14] is adopted. The effect of XPM on the channel under observation (assumed to be CW) due to interfering channels is calculated at the end of the SMF/DCF fibre link. Statistical methods are applied to calculate the XPM-induced crosstalk. At the fibre input, channel 1 (the channel to be

tested) is a CW signal, and the optical power of channel 2 (interferer) is sinusoidally modulated at a frequency ω. The corresponding powers at the input of the fibre link ($z = 0$) are:

$$P_1(0,t) = P_{10}, P_2(0,t) = P_{2C} + P_{2m}\cos(\omega t + \theta) \quad (12)$$

where P_{2m} is the amplitude of the sinusoidal power modulation; θ is an arbitrary initial phase. The scope of our analysis is to derive the spectral distribution of the crosstalk (interference) on the channel under test due to the XPM-induced intensity modulation. The XPM-induced intensity fluctuation is calculated integrating the amplitude of the intensity fluctuation due to each frequency component of the interferer.

The total intensity fluctuation at the end of the SMF section is:

$$\tilde{P}_{XPM}(\omega) = 2\gamma_1 P_{10}\tilde{P}_2(\omega)\, e^{-aL}e^{-i\omega L/v_{g1}} \left\{ \frac{\alpha\cdot\sin(bL) - (b+q)\cdot\cos(bL)}{\alpha^2+(b+q)^2} + \right.$$

$$\frac{[\alpha\cdot\sin(qL) + (b+q)\cdot\cos(qL)]\cdot e^{-\alpha L}}{\alpha^2+(b+q)^2} +$$

$$\frac{1}{\alpha^2+(b-q)^2}[\alpha\cdot\sin(bL) - (b-q)\cdot\cos(bL)$$

$$\left. - [\alpha\cdot\sin(qL) - (b-q)\cdot\cos(qL)]\cdot e^{-\alpha L}] \right\} \quad (13)$$

where $\alpha = a - i\omega d_{12}$. The previous analysis can be generalized in the case of a cascaded optical amplifier system of total length L_T consisting of $M-$segment fibre links. For the k^{th} wavelength channel, $L^{(l)}$, $a^{(l)}$, $D_k^{(l)}$, $\gamma_k^{(l)}$, and $g_k^{(l)}$ are the length and the attenuation coefficient, the dispersion coefficient, and the nonlinear coupling coefficient of the l^{th} fibre segment, respectively, and $g_k^{(l)}$ the gain of the l^{th} optical amplifier. The total XPM-induced crosstalk on the test channel n due to channel k is obtained adding up the contributions from all fibre sections and is given by:

$$P_{XPM,nk}(\omega) = 2P_{n0}P_k(\omega)\exp\left[-i\omega\sum_{l=1}^{N}\frac{L^{(l)}}{v_{gn}^{(l)}}\right]\sum_{l=1}^{N}\gamma_n^{(l)} \exp\left[i\omega\sum_{m=1}^{l-1}d_{nk}^{(m)}L^{(m)}\right]\prod_{m=1}^{l-1}e^{-a^{(m)}L^{(m)}}g_k^{(m)}\cdot$$

$$\left\{ \frac{\alpha_{nk}^{(l)}\sin\left(B_n^{(l-1)} - Q_k^{(l)}\right) - \left(b_{nk}^{(l)} + q_k^{(l)}\right)\cos\left(B_n^{(l-1)} - Q_k^{(l)}\right)}{\left(\alpha_{nk}^{(l)}\right)^2 + \left(b_n^{(l)} + q_k^{(l)}\right)^2} + \right.$$

$$\left. \frac{\left[\alpha_{nk}^{(l)}\sin\left(Q_k^{(l+1)} - B_i^{(l)}\right) + \left(b_n^{(l)} + q_k^{(l)}\right)\cos\left(Q_k^{(l+1)} - B_n^{(l)}\right)\right]e^{-\alpha_{nk}^{(l)}L^{(l)}}}{\left(\alpha_{nk}^{(l)}\right)^2 + \left(b_n^{(l)} + q_k^{(l)}\right)^2} + \right.$$

$$\left. \frac{\alpha_{nk}^{(l)}\sin\left(B_n^{(l-1)} + Q_k^{(l)}\right) - \left(b_n^{(l)} - q_k^{(l)}\right)\cos\left(B_n^{(l-1)} + Q_k^{(l)}\right)}{\left(\alpha_{nk}^{(l)}\right)^2 + \left(b_n^{(l)} - q_k^{(l)}\right)^2} \right.$$

$$\left. \frac{\left[\alpha_{nk}^{(l)}\sin\left(Q_k^{(l-1)} + B_n^{(l)}\right) - \left(b_n^{(l)} - q_k^{(l)}\right)\cos\left(Q_k^{(l+1)} + B_n^{(l)}\right)\right]e^{-\alpha_{nk}^{(l)}L^{(l)}}}{\left(\alpha_{nk}^{(l)}\right)^2 + \left(b_n^{(l)} - q_k^{(l)}\right)^2} \right\} \quad (14)$$

where

$$Q_k^{(l)} = \omega^2\lambda_k^2\sum_{m=1}^{l-1}L^{(m)}D_k^{(m)}/(4\pi c),$$

$$b_n^{(l)} = \omega^2 D_n^{(l)}\lambda_n^2/(4\pi c),\ q_k^{(l)} = \omega^2 D_k^{(l)}\lambda_k^2/(4\pi c),$$

and:

$$B_n^{(l)} = \omega^2\lambda_n^2\sum_{m=l+1}^{N}L^{(m)}D_n^{(m)}/(4\pi c),$$

Similar to the definitions given above, $\alpha_{nk}^{(l)} = a^{(l)} - i\omega d_{nk}^{(l)}$ with $d_{nk}^{(l)}$ being the walk-off parameter between channels n and k in the l^{th} fibre segment given by $d_{nk}^{(l)} \equiv \left(v_{gn}^{(l)}\right)^{-1} - \left(v_{gk}^{(l)}\right)^{-1}$.

When more than two light waves co-propagate in the optical fibre, each interfering wave k modulates the phase of the test channel independently. Group velocity dispersion then converts the XPM-induced modulation to intensity fluctuations. The total power fluctuation in probe channel induced by XPM at the end of the link can be written as:

$$P_{XPM,n}(L_T,t) = \frac{1}{2\pi}\sum_{k\neq n}\int_{-\infty}^{+\infty}\tilde{P}_{XPM}(\omega)\cdot e^{i\omega t}d\omega \quad (15)$$

where the $\tilde{P}_{XPM}(\omega)$ is given by (14).

2.4 EDFA Modelling

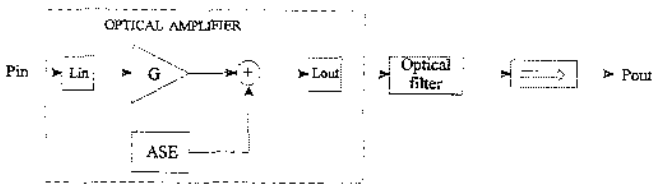

Figure 2. Block diagram of EDFA.

The block scheme of EDFA model is shown in Fig. 2 [17, 18]. Here we assume that the total output power of each amplifier is kept constant. For this case the gain G is the same for each node and can be determined by:

$$G = \frac{P_{s,0} + 2n_{sp}hfWL_{out}}{LL_{in}L_{out}P_{s,0} + 2n_{sp}hfWL_{out}} \quad (16)$$

where L is the fibre loss, L_{in}, L_{out} are the input and output connector losses, $P_{s,0}$ is the fibre input power, n_{sp} is the spontaneous emission factor, and f is the optical carrier frequency. The ASE power is $P_{ASE} = 2n_{sp}(G-1)h\nu W$ after the optical filter of bandwidth $W \cong \frac{c}{\lambda^2}(N-1)\Delta\lambda + R_b$, where N is the number of channels, $\Delta\lambda$ is the channel spacing, and R_b is the bit-rate.

3. Performance Evaluation

For evaluating the performance of a point-to-point system, the Q-factor has been used as a figure of merit.

Bit error probability (of the observed channel n) can be calculated using the Gaussian approximation [19]:

$$BER(n) = \frac{1}{4}\left[erfc\left(\frac{RP_1(n) - i_{tsh}}{\sigma_1(n)\sqrt{2}}\right) + erfc\left(\frac{i_{tsh} - RP_0(n)}{\sigma_0(n)\sqrt{2}}\right)\right] \quad (17)$$

where R is the photodiode responsivity, P_i(n) and $\sigma_i(n)$ (i= 0,1 denotes the space- and mark-state bits, respectively) are the signal power incident to photodiode and standard deviation of the n^{th} channel determined, respectively, by:

$$P_0(n) = rP_{s,M}(n)\,[1 - d_p(n)]\,, \qquad P_1(n) = P_{s,M}(n)\,[1 - d_p(n)]$$

$$\sigma_i(n) = \sqrt{\sigma_{th}^2 + \sigma(n)_{shot}^2 + \sigma(n)_{sig-spon}^2 + \sigma_{spon-spon}^2 + \sigma(n)_{sig-nl}^2} \quad (18)$$

with $P_{s,M}(n)$ being the nth bit signal power signal after the M^{th} amplifier and $d_p(n)$ the dispersion penalty for this channel. i_{tsh} is the decision threshold, and the error function is defined as:

$$erfc(x) = \frac{2}{\sqrt{\pi}}\int_x^{+\infty} e^{-u^2}du$$

r denotes the extinction ratio defined as $r = P_0/P_1$.

The thermal and shot noises as well as the signal-spontaneous and spontaneous-spontaneous noise terms are given by:

$$\sigma_{th}^2 = (NEP \cdot R)^2 B_e$$

$$\sigma_i(n)_{sh}^2 = 2qRP_i(n)B_e$$

$$\sigma_i(n)_{sig-spon}^2 = 2R^2P_i(n)P_{ASE,M}^{ch}B_e/B_o \text{ and} \quad (19)$$

$$\sigma_{spon-spon}^2 = R^2\left(P_{ASE,M}^{ch}\right)^2(2B_o - B_e)B_e/B_o^2$$

where $P_{ASE,M}^{ch} = P_{ASE,M}B_o/W$ is the total ASE noise power per channel after the M^{th} amplifier, NEP is the noise equivalent power, R is the photodiode responsivity, q an electron charge, and B_e is the electrical filter bandwidth.

Finally, the beating term between the optical power crosstalk from the nonlinearities and the signal is calculated by $\sigma_i(n)_{sig-nl}^2 = 2RP_i(n)P_{FWM}(n) + P_{SRS}^2(n) + P_{XPM}^2(n)$ with P_{SRS}^n, P_{FWM}^n, and P_{XPM}^n being the induced optical power crosstalk attributed to the respective effects of the nth channel, calculated using the methodology presented in Section 2. The crosstalk terms due to the optical nonlinearities themselves, as well as the beating between the nonlinearities and the ASE noise, are considered negligible and were omitted.

The Q-factor is determined starting from expression (17) by:

$$BER = \frac{1}{2}erfc\left(\frac{Q}{\sqrt{2}}\right), \quad (20)$$

for optimum threshold.

Using the aforementioned methodology and formalism, we calculated the dependence of the Q-factor on the bit-rate, channel spacing, and total fibre length. In particular, the Q-factor for a point-to-point link of 200 km and 600 km with 32 channels spaced either 50 GHz or 100 GHz at both 2.5 Gb/s and 10 Gb/s was calculated as a function of channel index parameterized with the channel power. The results are presented in Figs. 3–7.

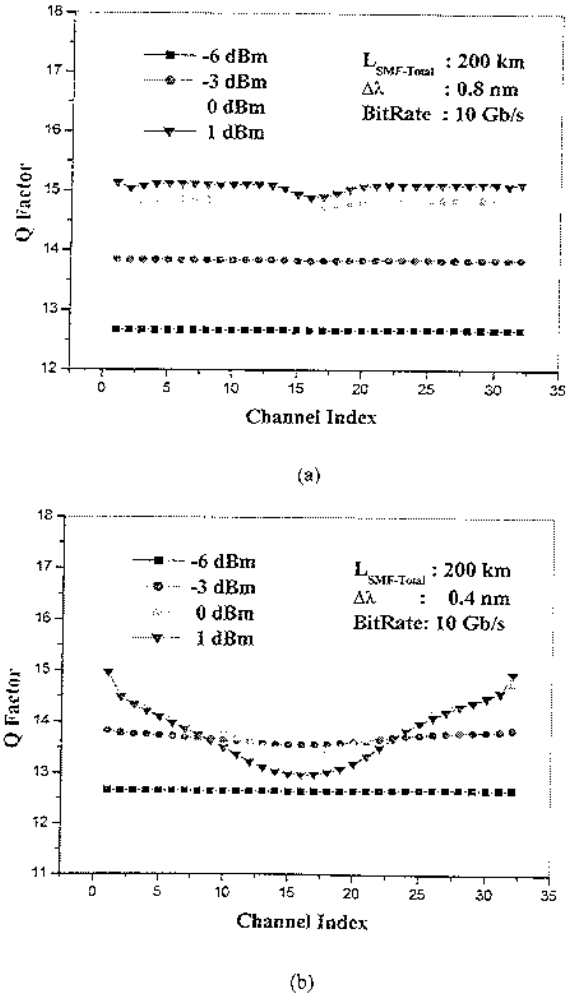

Figure 3. The Q-factor for a system with 200 km in length at 10 Gb/s (a) channel spacing 0.8 nm and (b) channel spacing 0.4 nm.

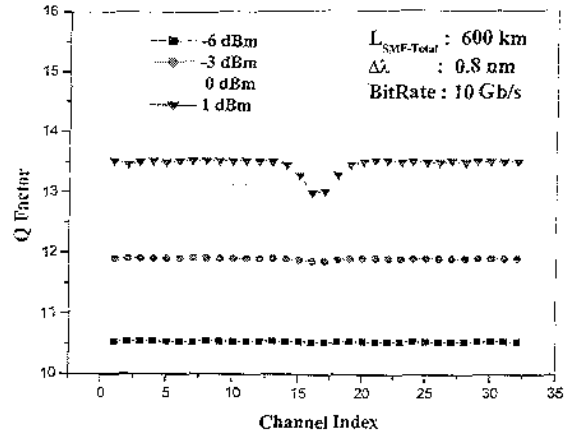

(a)

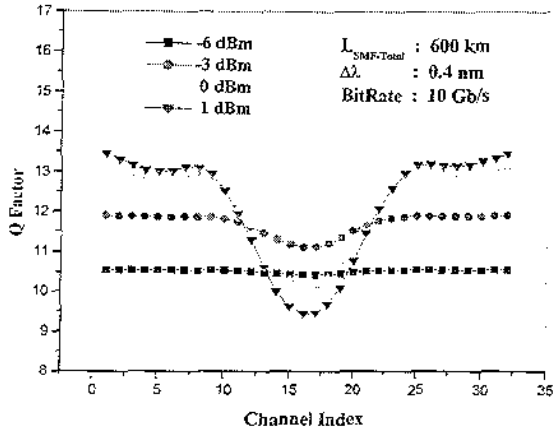

(b)

Figure 4. The Q-factor for a system with 600 km in length at 10 Gb/s (a) channel spacing 0.8 nm and (b) channel spacing 0.4 nm.

Figs. 3(a), (b) and 4(a), (b) illustrate the Q-factor of a system at 10 Gb/s versus the channel index for 200 km and 600 km, respectively. The SMF segment length used in analysis is 40 km. From these figures we deduce that the power per channel should be more than -6 dBm. From Figs. 3(b) and 4(b) we also see that the case with 0 dBm power per channel has better performance than the case of ± 1 dBm. This is already obvious at 200 km, but it is more profound at 600 km. This phenomenon is not observed in Figs. 3(a) and 4(a), indicating that XPM and FWM dominate over SRS in terms of performance degradation.

In Figs. 5 and 6(a), (b) the corresponding results are illustrated for a system modulated at 2.5 Gb/s. The best performance is obtained when the power per channel is –3 dBm. However, in all other cases the preferred power per channel strongly depends on the channel index, channel spacing, and total transmission length. This latter result is in line with our initial assumption, that parameter optimization should be carried out taking into consideration the major optical nonlinearities collectively, or incorrect conclusions could be drawn. For power levels 3 dBm per channel or higher the drop in Q-factor appears for the middle channels. Fig. 7 demonstrates the contribution of each nonlinearity separately on the Q-factor degradation as well as their relative strength. As expected, XPM and FWM mostly affect the system performance. Although that the deterministic part of SRS can be controlled by pre-emphasis techniques in each amplifier stage, the stochastic part cannot be controlled, and although SRS is not such an important factor for the distances considered here, it remains the important limiting factor in performance degradation for long-haul transmission. (More details on SRS crosstalk can be found in our recent article [9].)

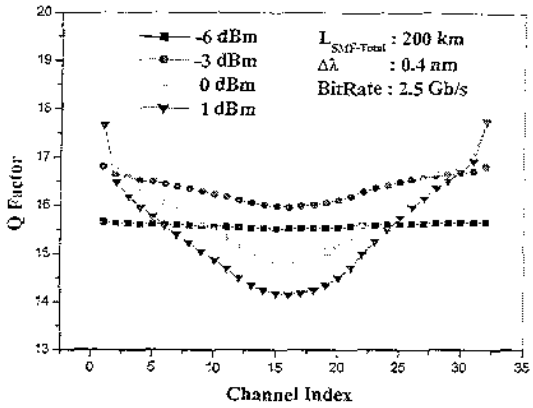

Figure 5. The Q-factor for a system with 200 km in length at 2.5 Gb/s and channel spacing 0.4 nm.

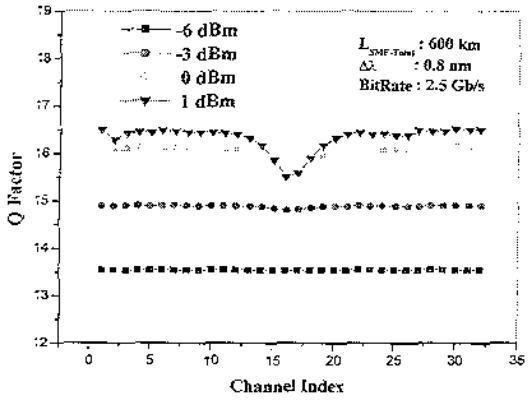

(a)

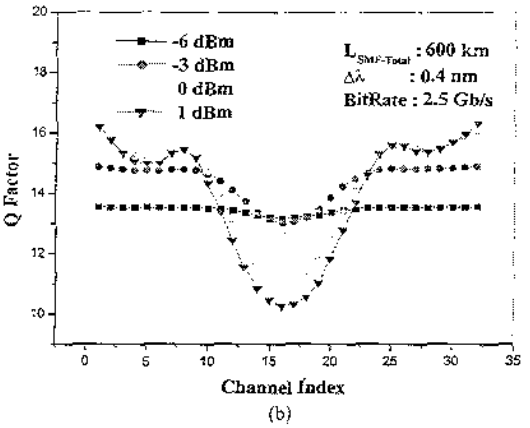

(b)

Figure 6. The Q-factor for a system with 600 km in length at 2.5 Gb/s (a) channel spacing 0.8 nm and (b) channel spacing 0.4 nm.

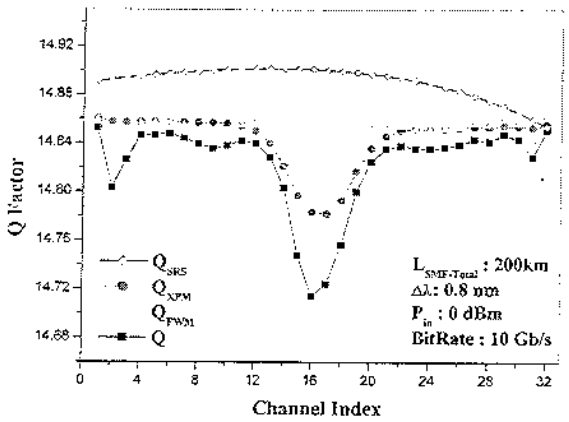

Figure 7. The strength of each nonlinearity on Q-factor degradation for a system with 200 km in length, at 10 Gb/s for average power per channel 0 dBm.

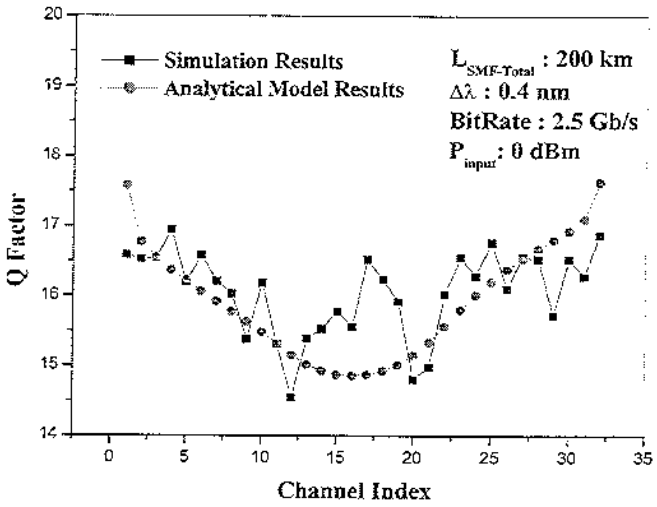

Figure 8. The comparison between the analytical model and numerical simulation results.

Finally, Fig. 8 shows the comparison between analytical model results and numerical simulation results. For the edge channels an excellent agreement is found, but for the middle channels there is some discrepancy. As the dispersion is nearly exactly compensated for the middle channels after every 40 km of SMF, the walk-off effect is not enough strong and FWM and XPM become more severe for those channels. Overall, the analytical models give very nice agreement with simulation results; they even predicted the effect of FWM resonance, considered in [17].

4. Conclusions

The analytic modelling of the collective influence of fibre nonlinearities on the Q-factor as well as their interplay with dispersion and ASE noise accumulation is an indispensable tool for studying wavelength-rich WDM networks. In this work the influence of SRS, FWM, and XPM on the Q-factor was studied for dispersion compensated optically amplified links comprised by alternate sections of SMF and DCF. The results suggested that the optimum selection of the power per channel could strongly depend on the other system parameters. The model we have developed can be used in designing advanced WDM systems with a large number of channels spanning many amplification bands where numerical simulations become impractically time consuming. The model gives satisfying results for MAN and WAN applications and submarine long-haul communications, which operate in so-called quasi-linear regime [17]. For much larger average power per channel usage (> 6 dBm), systems operate deeply in nonlinear regime, and the interplay among different nonlinearities and among nonlinearites and ASE noise become more complex and cannot be accurately predicted by analytical modelling, so that extensive numerical simulations are in that case unavoidable.

Acknowledgements

This work was partly funded by the European IST project DAVID, IST-1999-11742.

References

[1] S. Bigo, Where is the fun in designing 10 Tb/s transmission systems? *27th Conf. on Optical Communication 2001*, Tutorial Mo.M.2, September 30–October 4, 2001, Amsterdam.

[2] A. Stavdas, M. Manousakis, C. Scahill, & A. Hadjifotiou, Design and performance of free-space concave grating demultiplexers for ultrawideband WDM networks, *Journal of Lightwave Technology, 19*(11), 2001, 1777–1784.

[3] A. Stavdas, Architectural solutions toward a 1,000 channel ultra-wideband WDM network, *Optical Networks Magazine, 2*(1), 2001, 51–60.

[4] A. Yu & M.J. O'Mahony, Optimisation of wavelength spacing in a WDM transmission system in the presence of fibre nonlinearities, *IEE Proc. Optoelectronics, 142*(4), 1995, 190–196.

[5] X.Y. Zou, M.I. Hayee, S.-M. Hwang, & A.E. Willner, Limitations in 10 Gb/s WDM optical-fiber transmission when using a variety of fiber types to manage dispersion and nonlinearities, *Journal of Lightwave Technology, 14*(6), 1996, 1144–1152.

[6] M.I. Hayee & A.E. Willner, Pre- and post-compensation of dispersion and nonlinearities in 10-Gb/s WDM systems, *IEEE Photonics Technology Letters, 9*(9), 1997, 1271–1273.

[7] D.N. Christodoulides, Evolution of stimulated Raman crosstalk in wavelength division multiplexed systems, *IEEE Photonics Technology Letters, 8*(12), 1996, 1722–1724.

[8] K.-P. Ho, Statistical properties of stimulated Raman crosstalk in WDM systems, *Journal of Lightwave Technology, 18*(7), 2000, 915–921.

[9] I.B. Djordjevic & A.S. Stavdas, Analytical modeling of stimulated Raman scattering in WDM systems with dispersion compensated links, *Journal of Optical Communications, 24*(2), 2003, 54–60.

[10] K.O. Hill, D.C. Johnson, B.S. Kawasaki, & R.I. MacDonald, CW three-wave mixing in single-mode optical fibers, *Journal of Applied Physics, 49*, 1978, 5098–5106.

[11] K. Inoue, Four-wave mixing in an optical fiber in the zero-dispersion wavelength region, *Journal of Lightwave Technology, 10*(11), 1992, 1553–1561.

[12] I.B. Djordjevic & A. Stavdas, Probability density function of four wave mixing crosstalk in WDM systems, *Journal of Optical Communications, 22*(6), 2001, 236–238.

[13] W. Zeiler, F. Di Pasquale, P. Bayvel, & J.E. Midwinter, Modeling of four-wave mixing and gain peaking in amplified WDM optical communication systems and networks, *Journal of Lightwave Technology, 14*(9), 1996, 1933–1942.

[14] A.V.T. Cartaxo, Cross-phase modulation in intensity modulation-direct detection WDM systems with multiple optical amplifiers and dispersion compensators, *Journal of Lightwave Technology, 17*(2), 1999, 178–190.

[15] K.-P. Ho, E. Kong, L.Y. Chan, L.-K. Chen, & F. Tong, Analysis and measurement of root-mean-squared bandwidth of cross-phase modulation induced spectral broadening, *IEEE Photonics Technology Letters, 11*, 1999, 1126-1128.

[16] A.V.T. Cartaxo, Impact of modulation frequency on cross-phase modulation effect in intensity modulation-direct detection WDM systems, *IEEE Photonics Technology Letters, 10*(9), 1998, 1268–1270.

[17] E.A. Golovchenko, A.N. Pilipetskii, N.S. Bergano, C.R. Davidson, F.I. Khatri, R.M. Kimball, & V.J. Mazurczuk, Modeling of transoceanic fiber-optic WDM communication systems, *IEEE Journal of Selected Topics in Quantum Electronics, 6*(2), 2000, 337–347.

[18] C.R. Giles & E. Desurvire, Propagation of signal and noise in concatenated erbium-doped fiber optical amplifiers, *Journal of Lightwave Technology, 9*(2), 1991, 147–154.

[19] R.A.A. Lima, M.C.R. Carvalho, & L.F.M. Conrado, On the simulation of digital optical links with EDFA's: An accurate method for estimating BER through Gaussian approximation, *IEEE Journal of Selected Topics in Quantum Electronics, 3*(4), 1997, 1037–1044.

[20] G. Jacobsen, K. Bertilson, & Z. Xiaopin, WDM transmission system performance: Influence of non-Gaussian detected ASE noise and periodic DEMUX characteristic, *Journal of Lightwave Technology, 16*(10), 1998, 1804–1812.

Biographies

Ivan B. Djordjevic received his B.Sc., M.Sc., and Ph.D. degrees in electrical engineering from the Faculty of Electronic Engineering, University of Nish, Serbia, in 1994, 1997 and 1999, respectively. He has been associated with the University of Nish, Serbia; State Telecommunications Company, District Office for Networks in Nish, Serbia; National Technical University of Athens, Greece; TyCom US Inc., USA; and University of Arizona, USA. He is now with the University of Bristol, UK. He is the author of more than 60 publications in international journals and conference proceedings. His research interests include DWDM fibre optic communication systems and networks, error control coding for optical communications, optical CDMA systems, coherent optical communications, information theory, and statistical communication theory.

Alexandros Stavdas holds a B.Sc. in physics from the University of Athens, a M.Sc. in optoelectronics and laser devices from the Heriot-Watt University/St. Andrews University, and a Ph.D. from the University College of London in the field of wavelength routed WDM networks. He has worked on the design of free-space and integrated optics multiplexers/demultiplexers, wavelength cross-connects, and issues related to optical switching and wavelength routing systems. He was also technical leader for NTUA on the ACTS Project AC069 COBNET, on alternative ring architectures and in design considerations and scalability of WDM rings, and on AC050 PLANET in the area of generic architectures for the WDM upgrade of SuperPONs. Current interests include physical layer modelling of optical networks, ultra-high-capacity end-to-end optical networks, OXC architectures, WDM access networks, and optical packet switching. He is technical leader for NTUA on the IST Project DAVID. He is the author or co-author of several journal publications and conference presentations.

Charalampos Skoufis obtained his B.Sc. in physics from the Physics Department of the University of Athens. Following this he attended graduate courses in telecommunication at the Physics Department and Information Department of the University of Athens, and obtained his M.Sc. degree in 1999. His diploma thesis involved studies on the mode structure of VCSELs structures. He has been a Ph.D. student in electrical engineering at the National Technical University of Athens since 1999. His research topic concerns optical packet switching and simulations of optical components.

Stelios Sygletos obtained his diploma in electrical engineering and computer science from the Department of Electrical Engineering and Computer Science of the National Technical University of Athens, Greece, with specialization in telecommunications. His diploma thesis concerned the development of models for the simulation of the switching behaviour of a semiconductor optical amplifier. Mr. Sygletos has been a member of the technical staff of PCRL for two years and was recently accepted into the postgraduate program of the Department leading to a Ph.D. His research topic concerns all-optical signal regeneration. Mr. Sygletos was awarded a prize in the annual national contest of the Greek Mathematical Union.

Chris Matrakidis has an electrical engineering degree from the University of Patras and a Ph.D. from University College London in the field of digital communications. From 1995 to 1999 he was a Research Fellow at the Telecommunications Research Group of UCL. His primary research interests are in the areas of simulation and optimization of communication systems. He has also worked on applications of coding theory, GSM systems, optical networking, satellite communications, and magnetic recording. He is author or co-author of several journal and conference publications.